CONFERENCE PRE-PRINT

CORE-LOCALIZED ELECTROMAGNETIC INSTABILITY IN THE PLASMA WITH A WEAK MAGNETIC SHEAR ON THE HL-2A TOKAMAK

P. W. Shi¹, W. Chen¹, J. Q. Xu¹, R. R. Ma¹, L. M. Yu¹, M. Jiang¹, X. Yu¹, X. X. He¹, Z. C. Yang¹, L. W. Hu¹, Z. B. Shi¹ and W. L. Zhong¹

¹Southwestern Institute of Physics, P.O. Box 432 Chengdu 610041, China

Corresponding Author: shipw@swip.ac.cn

Abstract:

Recently, Alfvénic ion temperature gradient (AITG) modes are observed in the HL-2A plasma with weak magnetic shear. Only when electron cyclotron resonance heating (ECRH) and neutral beam injection (NBI) are simultaneously injected into the deuterium plasma, AITG modes become unstable. The instability is electromagnetic and localized in the core plasma with an internal transport barrier. Dynamic evolution of AITG modes are greatly affected by the off-axis ECRH. Numerical and theoretical analysis suggests that there is a strong dependence of the AITG modes on $\eta_i \simeq \nabla \ln T_i/\nabla \ln n_i$. More interesting, it is also found that ECRH can enhances AITG modes by causing an increase in $\tau = T_e/T_i$, here T_e and T_i are electron and ion temperature, respectively. Besides, high-power ECRH may also change safety factor and then contribute to mitigation of AITG modes.

Introduction—Core-localized electromagnetic modes can be driven unstable by large pressure gradient formed in region of weak magnetic shear. Actually, the first threshold of pressure gradient becomes much smaller in case of weak magnetic shear, and it enables destabilization of electromagnetic instability with a low toroidal mode number[1]. Alfvénic ion temperature gradient (AITG) mode, one of typical pressure gradient driven electromagnetic modes, is firstly predicted in theory. When ion compression effect couples to shear Alfvén wave in plasma with finite ∇T_i effect, the AITG mode induced by kinetic wave particle interactions with thermal ions, may become unstable with a very low threshold $\beta_{AITG} \leq 0.4 - 0.5\beta_{crit}$. Here, β_{crit} refers to the marginal stability boundary of ideal magnetohydrodynamic ballooning modes. It can also be excited in the plasma with a condition of $\Omega_{*pi} \sim q\sqrt{7/4} + \tau$, and usually regarded as a branch connecting the kinetic ballooning mode (KBM, diamagnetic effect is dominant, $\Omega_{*pi} \gg q\sqrt{7/4+\tau}$) and beta induced Alfvén eigenmode (BAE, ion compression effect is dominant, $\Omega_{*pi} \ll q\sqrt{7/4+\tau}$) [2]. Here, q is safety factor and $\tau = T_e/T_i$. It was reported that the stability of AITG modes has a strong and complex dependence on multiple effects, including magnetic shear, pressure gradient, trapped electrons, Shafranov shift as well as parallel ion current. A theoretical framework for the AITG mode had been well developed[3], but experimental evidences for the core-localized electromagnetic modes are rather limited. It was firstly experimentally validated in HL-2A plasma with peaked density profiles and weak magnetic shear [4]. The AITG modes were also observed in high ion temperature and high- β plasmas. Only a few experimental evidences for the AITG modes were presented nowadays, but they were found to cause minor disruption and expected to affect thermal electron transport, which will become a major concern in the future burning plasma with Alpha particle heating. Besides, the AITG modes may also be unstable in magnetically confined plasma with reactor-relevant parameters. As the first plasma of ITER getting closer, better systematical understanding for the electromagnetic instability via combination of theory and experiment become more and more urgent.

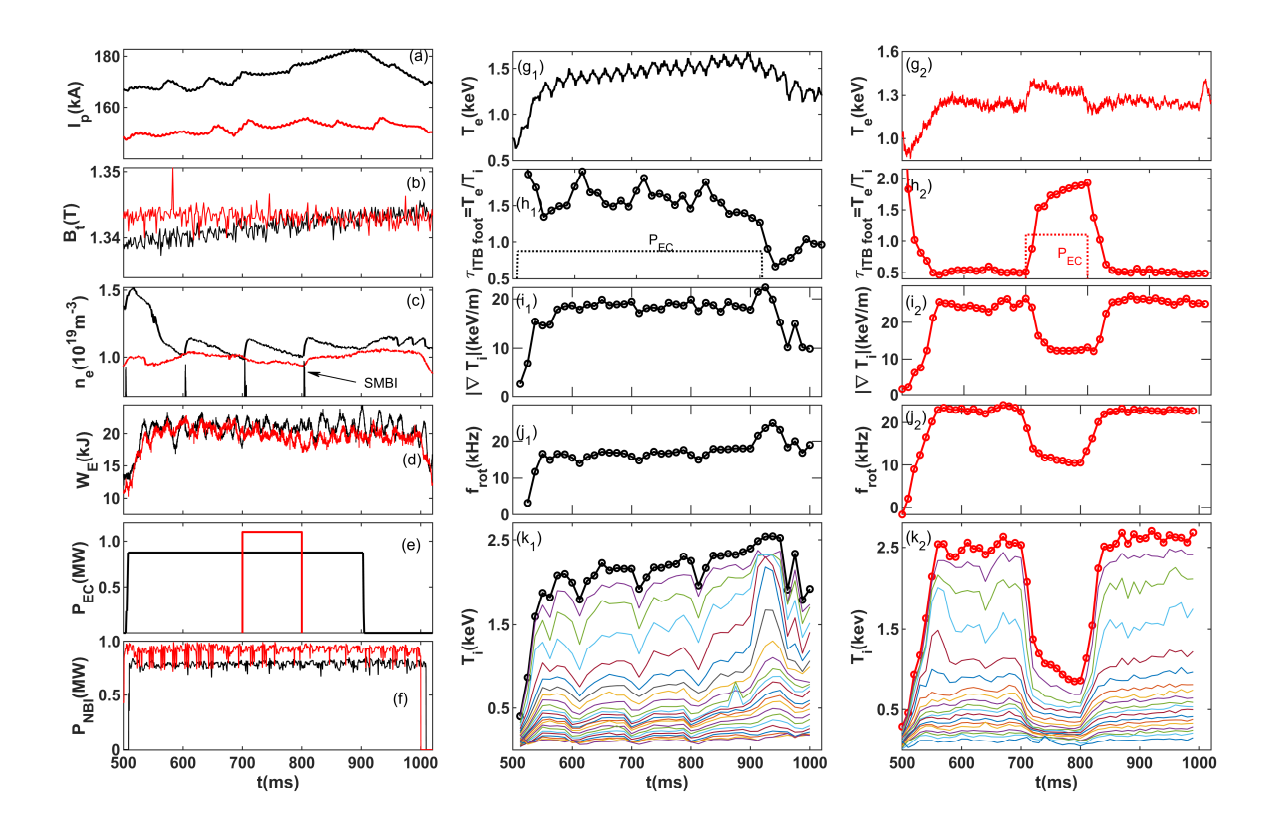


FIG. 1: Temporal evolution of (a) plasma current, (b) magnetic field, (c) line-averaged electron density, (d) plasma stored energy, (e) power of electron cyclotron resonance heating, (f) power of neutral beam injection, (g) electron temperature at magnetic axis, (h) ratio of electron and ion temperature at the ITB foot, (i) maximum ion temperature gradient, (j) rotation frequencies and (k) ion temperature for the 26006 (black) and 27527 (red) discharges, which are distinguished by the subscripts of '1' and '2' in subgraph (g-k).

Experimental observation and theoretical analysis of AITG modes.—The experiments for AITG modes are performed in divertor configuration. Figure 1 shows the basic parameters during two typical discharges of 26006 and 27527. Plasma current I_p , toroidal magnetic field B_t , line-averaged electron density n_e , stored energy W_E and injected power of ECRH and NBI are given at the first six subgraphs. The electron temperature T_e , ratio of electron and ion temperature ($\tau = T_e/T_i$) in the ITB foot, ion temperature T_i and rotation frequency f_{rot} are plotted at Fig.1(j-k), where the subscripts of '1' and '2' represent data from 26006 and 27527 discharges, respectively. It should be noted that when ECRH is injected into plasma, drops in T_i and n_e , moderate growth of T_e appear in core region during the 27527 discharge. But a different tendency can be observed when RF wave is turn off during the 26006 discharge. In other words, ECRH is responsible for an increase of $\tau = T_e/T_i$ in Fig.1. Spectrograms measured by microwave interferometer, soft X-ray array and Mirnov coil are given in Fig.2. Different responses are found

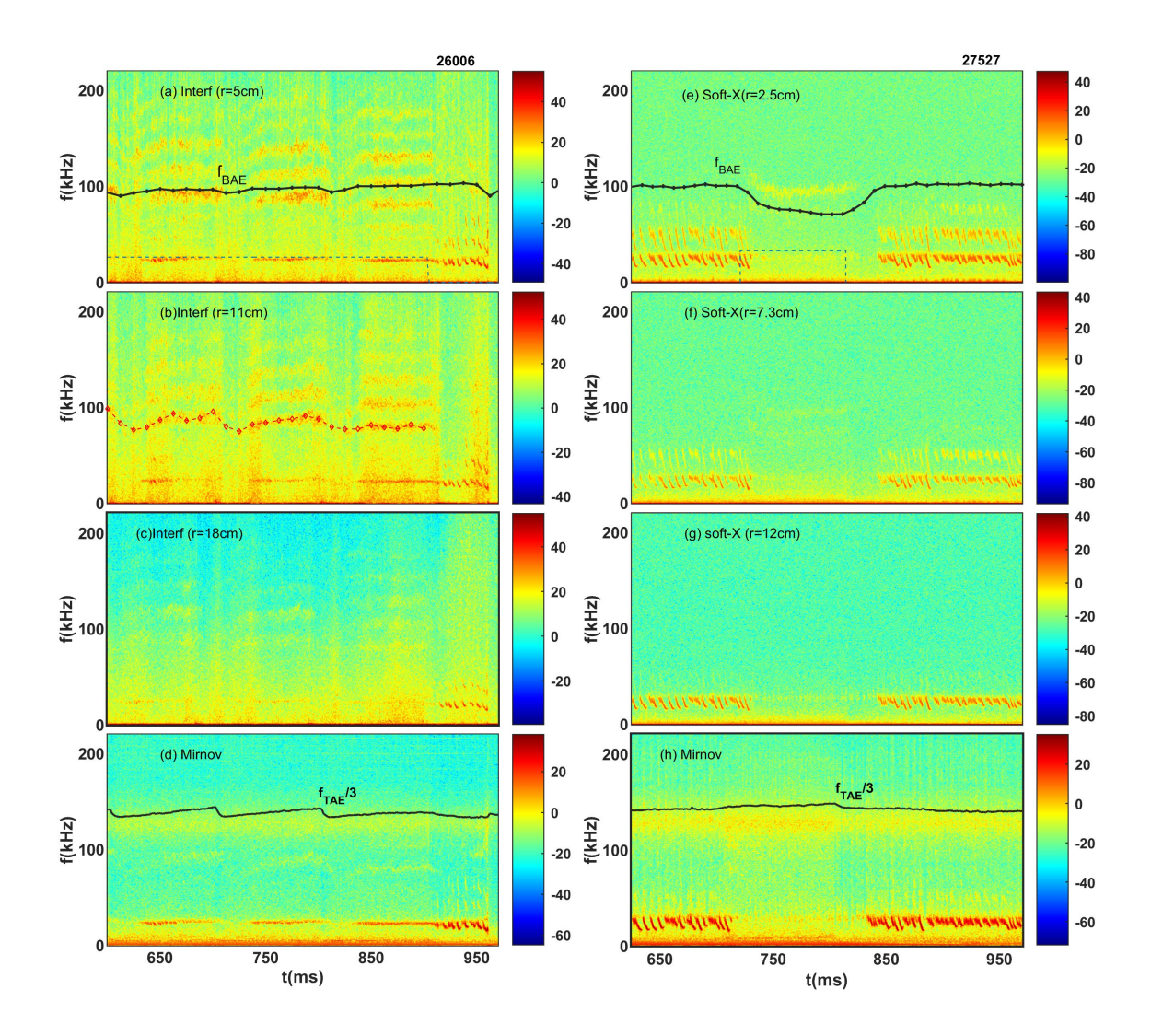


FIG. 2: Spectrograms during the 26006 (left column) and 27527 (right column) discharges. Those spectrograms are measured by (a-c) microwave interferometer, (e-g) soft X-ray array, (d) and (h) Mirnov probe in midplane. The blue curves in (a) and (e) are the waveforms of ECRH. The black curves in (a) and (e) are the BAE frequency given by $f_{BAE} = \frac{1}{2\pi} \sqrt{7/4 + T_e/T_i} \sqrt{2T_i/m_i}$ and that in (d) and (h) are a third of TAE frequency by $f_{TAE} = V_A/4\pi q R_0$ with $B_t = 1.34T$, $n_e = 1.0 \times 10^{19} m^{-3}$ and q = 1.5.

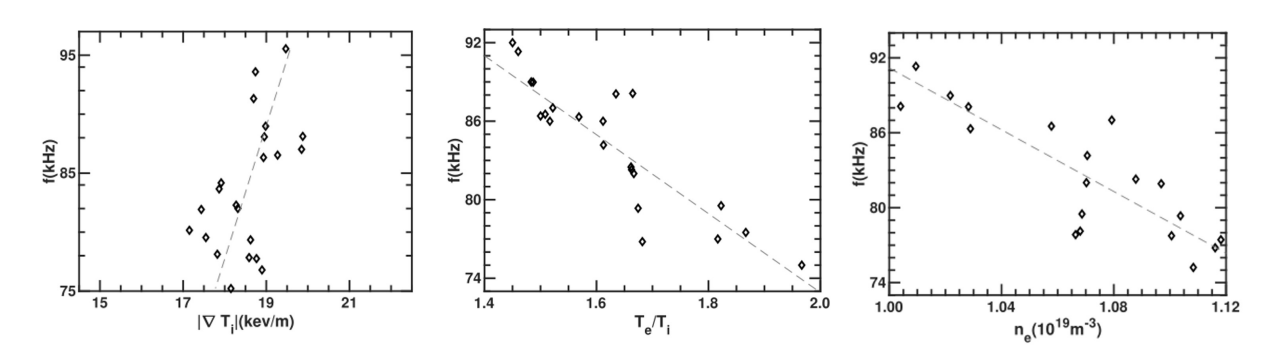


FIG. 3: Dependence of mode frequency on the maximum ion temperature gradient $|\nabla T_i|$, T_e/T_i and line-averaged electron density n_e .

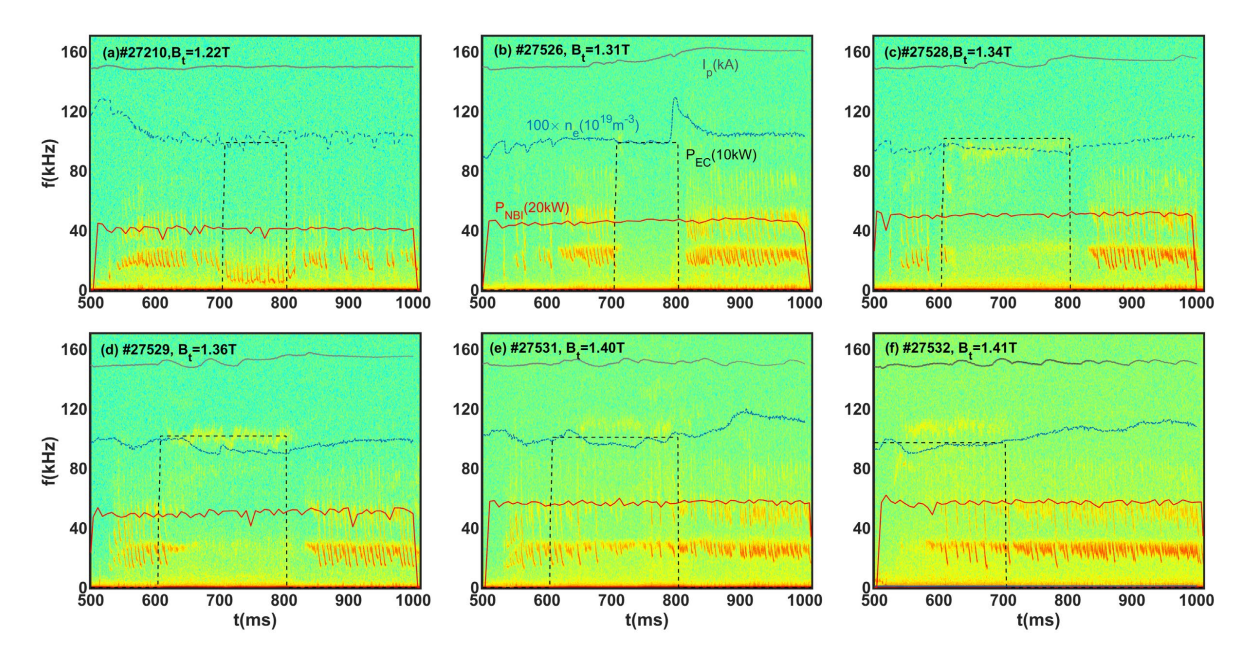


FIG. 4: Spectrogram obtained from the r=2.5 channel on soft X-ray array in six different discharges of (a) 27210 with $B_t=1.22$ T and $\rho_{EC}=0.02$, (b) 27526 with $B_t=1.31$ T and $\rho_{EC}=0.32$, (c) 27529 with $B_t=1.34$ T and $\rho_{EC}=0.427$, (d) 27529 with $B_t=1.36$ T and $\rho_{EC}=0.6$, (e) 27531 with $B_t=1.4$ T and $\rho_{EC}=0.63$, (f) 27532 with $B_t=1.41$ T and $\rho_{EC}=0.66$. The gray, blue, black and red curves are waveforms of $I_p(kA)$, $100 \times n_e(10^{19}m^{-3})$, power of ECRH and NBI, i.e. $P_{EC}(10kW)$ and $P_{NBI}(20kW)$.

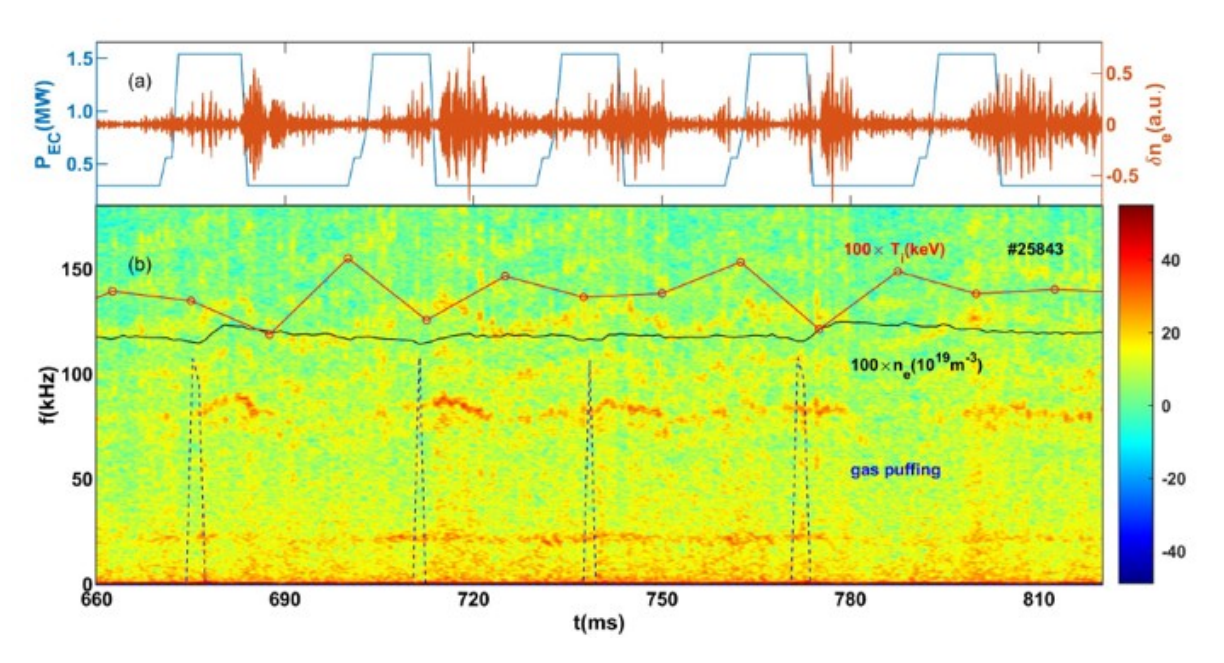


FIG. 5: Effect of ECRH on electromagnetic modes during 25843 discharge: waveform of ECRH and density fluctuation obtained from a numerical filter with a frequency of (a) 80-90 kHz; spectrogram given by microwave interferometer are arranged in (b).

on the three diagnostics due to different sensitivities and installation locations. There are two kinds of instabilities during simultaneous injection of NBI and ECRH. The lower frequency (< 50kHz) one is long-lived mode or fishbone mode and its second harmonic, the other one with a higher frequency is electromagnetic and locates at the core region. First of all, the high frequency mode can be measured by Mirnov probe and microwave interferometer. The former reveals a magnetic perturbation while the latter presents a density fluctuation, which is proportional to electrostatic perturbation. It is worthy noting that the mode has a larger amplitude in low field side then high field side. Those results mean that the modes are electromagnetic and have a typical ballooning mode structure. Then, different responses of electromagnetic instability at different channels of microwave interferometer and soft X-ray array enable determination of mode location. In the 26006 discharge, six modes with toroidal mode number of $n=1\sim 6$ can be detected by the r = 5cm channel on microwave diagnostics, but less modes with weaker fluctuation level by both r = 11cm and r = 18cm channels. Such a result indicates a core location for the electromagnetic mode. During the 27527 discharge, only the n=3 mode can be detected by the two channels of soft X-ray array at r = 2.5cm and r = 7.3cm, but not by other channels in outer region, just shown as Fig.2(e-g). So we can come to that the mode is localized at region nearby $r \leq 7.3cm$ ($\rho \leq 0.18$). The experimental mode frequency ranges from 70kHz to 200kHz and is much lower than TAE frequency given by $f_{TAE} = V_A/4\pi q R_0 \simeq 450 kHz$ with $B_t = 1.34T$, $n_e = 1.0 \times 10^{19} m^{-3}$ and q = 1.5. So TAE can be excluded from the mode identification. Actually, the experimental mode frequency is comparable to BAE frequency $(f_{BAE} = \frac{1}{2\pi}\sqrt{7/4 + T_e/T_i}\sqrt{2T_i/m_i})$ and the electromagnetic modes may belong to KBM/AITG/BAE. According to theoretical prediction, it will be a KBM if diamagnetic effect is dominant $(\Omega_{*pi} \gg q\sqrt{7/4+\tau})$, be a BAE if ion compression effect is dominant $(\Omega_{*pi} \ll q\sqrt{7/4+\tau})$ and be a AITG mode if $\Omega_{*pi} \sim q\sqrt{7/4+\tau}$. Figure 3 present the dependence of mode frequency on maximum ion temperature gradient $|\nabla T_i|$, T_e/T_i and line-averaged electron density n_e . The experimental frequency is in directly proportional to $|\nabla T_i|$. However, the mode frequency will decline with an increasing of T_e/T_i or n_e . Those statistical results may indicate that the modes are driven by ion temperature or pressure gradient rather than energetic particles.

To further reveal relationship between ECRH and the interesting modes, deposition locations of ECRH are changed by a B_t scan while the ECRH power is fixed as 1000kW. Other parameters also keep unchanged during the B_t scan experiment. The plasma current is set as $I_p \simeq 150kA$, electron density is remained as $n_e \simeq 1.0 \times 10^{19} m^{-3}$ and NBI system is operated with a power of $P_{NBI} \simeq 800 - 1100kW$ during t = 500 - 1000ms. The results are given in Fig.4. Interestingly, the electromagnetic instability is driven unstable only when ECRH and NBI are simultaneously injected into the plasma with $B_t \geq 1.34T$ (the corresponding deposition location of 68GHz ECRH is about $\rho \leq 0.427$). Decline in n_e and weak perturbation in I_p appear during injection of ECRH. The former is caused by the pump-out effect of RCEH while the latter may indicate a change of safety factor. However, accurate q profiles are unavailable due to lack of motional Stark effect diagnostic or interferometer-polarimeter. It should be pointed out that temporal evolutions of T_e and T_i are similar to that during the typical discharges of 26006 and A power modulation experiment is also designed to find out ECRH power threshold for mode excitation, and the results are shown as Fig.5. There are 4 gyrotrons during experiment, where a gyrotron works with an unchanged power of 300kW while other three operates with a period of 30ms and a total power of 1200kW. The power threshold is proved to be very low, since electromagnetic modes can be detected in the

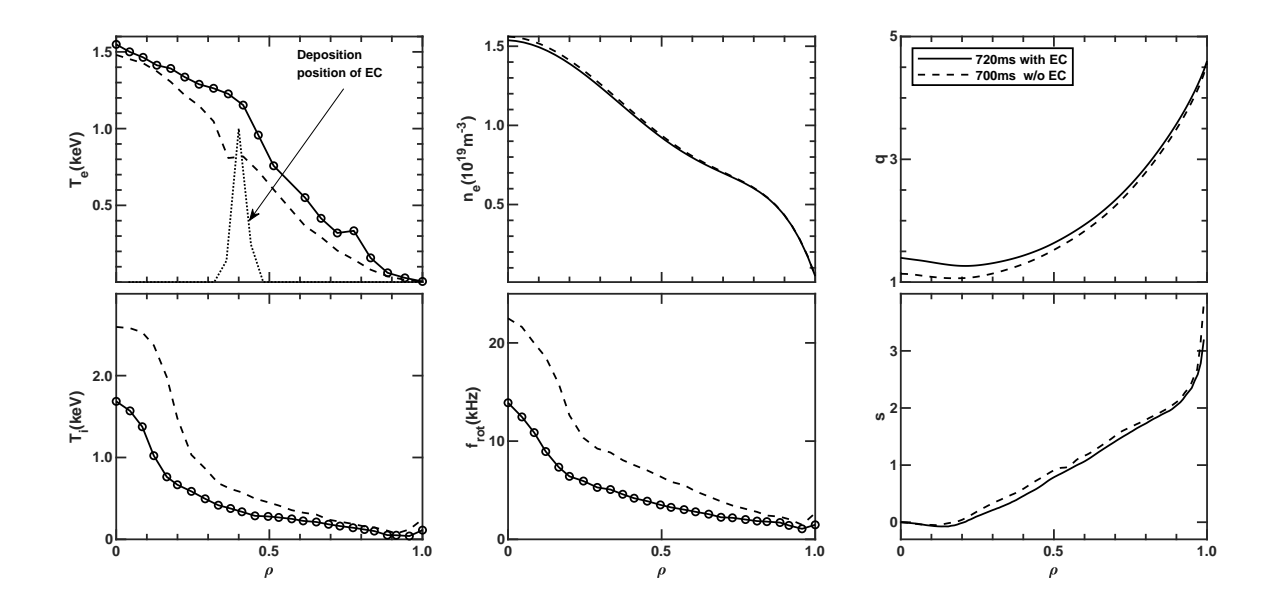


FIG. 6: Radial profiles of electron temperature, electron density, safety factor q, ion temperature, rotation frequency and magnetic shear s during the 27527 discharge. The solid and dotted curves are data at 700ms (without ECRH) and 720ms (with ECRH).

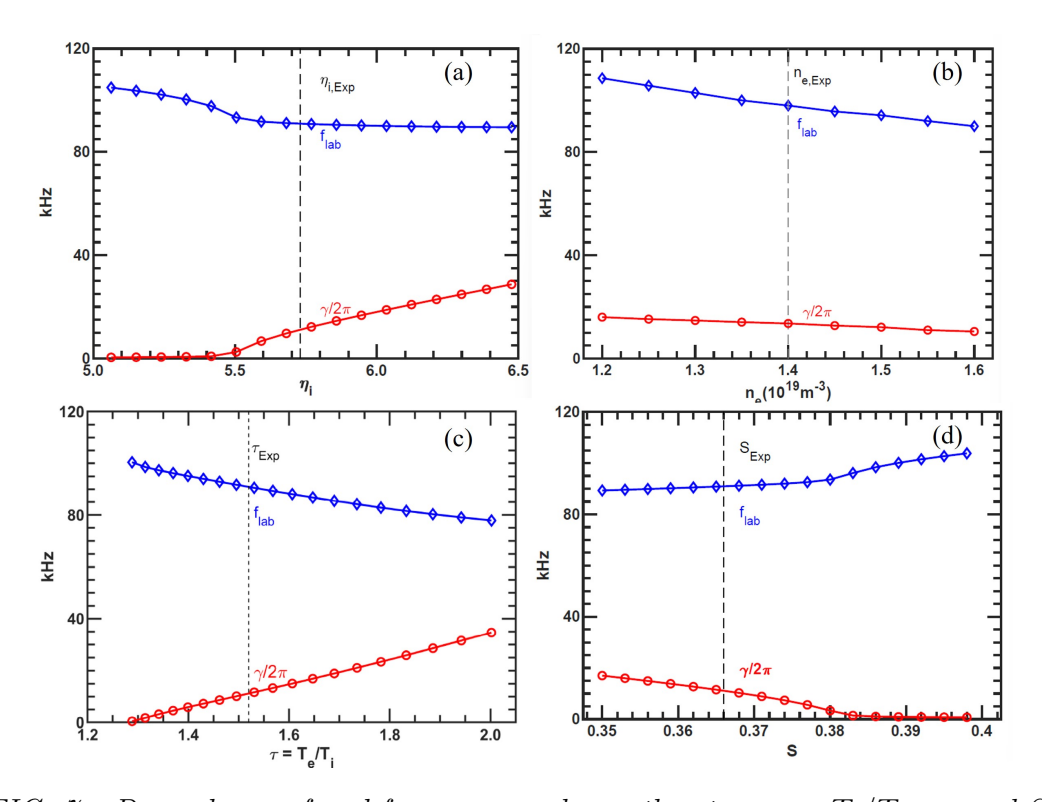


FIG. 7: Dependence of real frequency and growth rate on η_i , T_e/T_i , n_e and S.

two case of $P_{EC} = 300kW$ and $P_{EC} = 1500kW$. In the 25843 discharge, mode frequency of electromagnetic instability becomes higher accompanied with a drop of T_i and an increase in n_e induced by gap puffing and/or ECRH. Thus, those modes should be AITG modes rather than BAEs with $f_{BAE} \propto \sqrt{T_i}$. More interesting, mitigation effect of ECRH on AITG mode has been achieved in experiment. Density fluctuation (δn_e) induced by the electromagnetic instability becomes weaker (stronger) when the 1200kW ECRH is turned on (turned off). Low level of δn_e is found without 1200kW ECRH and an increase of δn_e can also be observed during radio-frequency heating. It may suggest a complex stabilization mechanism for the pressure gradient driven AITG modes. It should be noted that, a transition from long-lived mode to fishbone mode occurs when the high power RF wave is injected in a similar discharge (No.25845). Since positive and weak magnetic shears are favourable for the excitation of long-lived mode, but a reversed shear is more crucial for the fishbone modes. So the mode transition may indicate a change in safety factor or magnetic shear. In other words, the ECRH may mitigate AITG modes by firstly changing local T_e , T_i , n_e and plasma pressure, and then varying safety factor or magnetic shear via the Grad-Shafranov equation, which describes a coupling of current density and plasma pressure. The equilibrium profiles at 700ms (without ECRH) and 720ms (with ECRH) are shown as Fig.6. Here, T_e profile consists of data from ECE radiometer, n_e profile is obtained from a laser interferometer, T_i and f_{rot} are measured by a charge exchange recombination spectroscopy, q profile is reconstructed by ONETWO code based on the first four parameters. It is found that off-axis ECRH leads to great drops of T_i and f_{rot} at the core region and a noticeable growth of T_e at outer area. The two reconstructed q profiles also present a great difference, i.e. safety factor increases in the core when ECRH is launched into plasma. It may because the ECRH leads to drop in pressure gradient by changing n_e , T_e and T_i , then decline current density and improve the safety factor.

To explain experimental phenomenon, a brief theoretical analysis based on GFLDR has also been carried out. For local low-frequency shear Alfvén wave, the GFLDR can be wrote as[3]

$$iS(\Lambda_n^2 - k_{\parallel 0}^2 q_{min}^2 R_0^2)^{1/2} (1/n)^{1/2} [k_{\parallel 0} q_{min} R_0 - i(\Lambda_n^2 - k_{\parallel 0}^2 q_{min}^2 R_0^2)^{1/2}]^{1/2} = \delta W_f + \delta W_k \quad (1)$$

Here, $k_{\parallel 0} = (nq_{min} - m)/q_{min}R_0$, $S = (r/q)[q'']^{1/2}$ and q'' is the second derivative of safety factor, δW_f and δW_k are the fluid and kinetic contribution in regular ideal region. The generalized inertia term Λ_n , including both diamagnetic effects as well as kinetic effects of circulating and trapped particle dynamic, is given at reference [5]. For pressure gradient driven instability, the term of δW_k can be negligible. In low frequency limits $(0 < \omega < \omega_{ti})$, the δW_f is described as[?]

$$\delta W_{nf} \simeq \frac{\pi}{4} \left(\frac{S^2 k_{\parallel 0} q_{min} R_0}{n} - \frac{3}{2} \alpha^2 S \left| \frac{k_{\parallel 0} q_{min} R_0}{n} \right|^{1/2} + \frac{9}{32} \alpha^4 \right) \tag{2}$$

where $\alpha = -R_0 q^2 d\beta/dr$ and $\beta = \beta_i (1 + T_e/T_i)$.

For local calculation at 720ms during the 27527 discharge, numerical inputs are evaluated at $\rho \equiv r/a = 0.161$, where there are a minimum safety factor q_{min} and an ITB foot. The detail parameters are (m,n)=(4,3), $q_{min}=1.28$, $R_0=1.658m$, R=1.722m, s=-0.0017, $k_{\parallel 0}q_{min}R_0=-0.163$, $k_{\theta}\rho_i=0.273$, $k_{\theta}\rho_e=0.0056$, $\epsilon_i=0.304$, $\beta_i=0.29\%$, $\eta_i \equiv \nabla \ln T_i/\nabla \ln n_i=5.73$, S=0.366 and $\tau=1.52$. Here, ρ_i and ρ_e are larmor radius of ion and electron, respectively. The ion transit frequency $\omega_{ti} \equiv \sqrt{2T_i/m_i}/qR=3.417$,

the thermal ion diamagnetic drift frequency due to density gradient is $\omega_{*ni} = 0.596$ and $\omega_{*pi} = 4.01$. $\Omega_{*pi} = \omega_{*pi}/\omega_{ti} \simeq 1.17$ is comparable to $q\sqrt{7/4+\tau} \simeq 2.3$. Besides, δW_f is about -0.0162. Thus, the AITG mode can be unstable for $\delta W_f < 0$ in the absence of energetic particles. Dependence of real frequency and growth rate on η_i , T_e/T_i , n_e and S are shown in Fig.7. Firstly, beyond the critical threshold of $\eta_i \geq 5.4$, the growth rate becomes larger with an increase of η_i , but the mode frequency keeps almost fixed as 91kHz, which agrees well with experimental frequency of 96kHz. Secondly, it is found that there also is a threshold in T_e/T_i , which is about 1.28. When τ exceeds this value, the AITG modes become more unstable. The theoretical analysis provides a reasonable explanation for AITG modes excitation during the ECRH heating, which increases T_e directly and causes a drop in T_i . Thirdly, both f_{lab} and $\gamma/2\pi$ become lower when n_e grows up. It means that the AITG modes are more unstable in low density plasma. Further more, the frequency evolution given by theoretical calculation agrees well with experimental statistics in Fig.6. Finally, since AITG modes have the same location to that of minimum safety factor, S, instead of $s \simeq 0$ at one isolated singular, is used in the theoretical analysis. Growth rate and frequency exhibit different features with an increase of S. The former is directly proportional to S while the latter shows a reversed trend. The AITG modes will become stable when S reaches to the critical value of 0.383. It may indicate that one can mitigate or suppress those modes by active control of safety factor.

Summary.—Core-localized pressure gradient driven AITG modes are unstable in HL-2A plasma with simultaneously injection of NBI and off-axis ECRH. The ECRH is found to play an important role in the mode excitation and evolution by causing change in $|\nabla T_i|$, T_e/T_i and n_e . Further theoretical analysis based on GFLDR indicates that there are three thresholds of η_i , T_e/T_i and S for the mode excitation. In our experiments, the NBI heats thermal ions and improves ion temperature, then results in η_i exceeding the critical value of $\eta_{i,cri} \geq 5.4$. The off-axis ECRH enhances AITG modes mainly by increasing T_e and causing a drop in T_i . Besides, the ECRH can also lead to a low density by pump-out effect and drive the AITG modes. Last but not least, mitigation of AITG modes by ECRH is firstly achieved. The new findings in this paper can not only enrich experimental knowledge for pressure gradient driven instability, but also be beneficial to active control of core-localized electromagnetic modes in the future burning plasma.

References

- [1] A. Hirose and M. Elia, *Phys. Rev. Lett.* 76 628(1996).
- [2] F. Zonca et al., Plasma Phys. Control. Fusion 38 2011 (1996).
- [3] L. Chen and F. Zonca, Rev. Mod. Phys. 88 015008 (2016).
- [4] W. Chen et al., EPL 116 45003 (2016).
- [5] I. Chavdarovski et al., Plasma Phys. Control. Fusion 51 115001 (2009).